Journal of NeuroVirology, 13: 38–46, 2007

ISSN: 1355-0284 print / 1538-2443 online
DOI: 10.1080/13550280601145340

informa
healthcare

Aquaporin 4 regulation during acute and long-term experimental Herpes simplex virus encephalitis

FJ Martinez Torres,[1] D Völcker,[1] N Dörner,[1] Th Lenhard,[1] S Nielsen,[1] J Haas,[1] K Kiening,[2] and U. Meyding-Lamadé[1]

Departments of [1]Neurology and [2]Neurosurgery, University of Heidelberg, Heidelberg, Germany

Structural damage of the central nervous system (CNS) often leads to severely disabling residual symptoms despite effective antiviral therapy during Herpes simplex virus encephalitis (HSVE). Edematous space-occupying lesions are pathological and neuroradiological well-known phenomena for this disease. The molecular mechanisms of brain edema development in HSVE are poorly understood, the regulation of water brain-blood barrier (BBB) permeability might be disturbed. Aquaporin 4 (AQP4) is the predominant aquaporin expressed in the brain. Aquaporin 1 (AQP1) plays a role in cerebrospinal fluid modulation. Previous studies suggest that alterations of AQP expression play an important role in the development of brain edema. The mRNA expression of AQP4, AQP1, of their physiologically associated proteins Alpha-syntrophin and KIR 4.1 and of the structural glial protein glial fibrillary acid protein (GFAP) was analyzed in a well-established mice model simulating the human disease. Our data demonstrate a significant down-regulation of AQP4 in the acute phase of disease and an up-regulation of AQP4 and AQP1 in the long term. These results reveal the complex transcription pattern of AQP4, AQP1, KIR 4.1, alpha-syntrophin, and GFAP during HSVE and suggest a role for AQP4 regulation in the pathophysiology of acute and long-term HSVE. AQP4 modulation could be a potential target for brain edema treatment during HSVE. *Journal of NeuroVirology* (2007) **13,** 38–46.

Keywords: alpha-syntrophin; aquaporins, herpes simplex virus encephalitis; KIR 4.1; real-time PCR

Introduction

Herpes simplex virus (HSV) is the most common infectious agent responsible for sporadic acute encephalitis in central Europe and the United States (Steiner and Kennedy, 1995). The mortality rate is higher than 70% when the disease is left to its natural course. Mortality and the incidence of severe neurological deficits remain unacceptably high despite effective antiviral treatment (McGrath *et al*, 1997).

The limbic system and the insular cortex are the most affected areas of the brain during HSV encephalitis (HSVE). These areas are usually detected with cranial magnetic resonance imaging (MRI) as T2-weighted hyperintense lesions (Meyding-Lamadé *et al*, 1999a). Despite clinical recovery, patients with proven HSVE present chronic progressive structural damage with areas of abnormal signal intensity in cranial MRI. These findings support the hypothesis that virus-independent mechanisms might be responsible for structural damage in this devastating disease (Meyding-Lamadé *et al*, 1999a).

The involvement of virus-independent secondary mechanisms of neuronal and glia damage is part of ongoing research (Martinez-Torres *et al*, 2004). Acyclovir specifically inhibits viral replication and does not influence secondary mechanisms of damage (McGrath *et al*, 1997). A better understanding of the mediators of tissue damage in HSVE is essential in order to find new targets for therapeutic intervention.

A tight regulation of brain water content and volume is essential in order to assure the normal function of the central nervous system (CNS). Aquaporin

Address correspondence to F. J. Martinez Torres, Department of Neurology, University of Heidelberg, Im Neuenheimer Feld 400, 69120, Heidelberg, Germany. E-mail: francisco.martinez@med.uni-heidelberg.de

Received 18 August 2006; revised 17 October 2006; accepted 15 November 2006.

water channels have been recognized to play an essential role in cerebral water homeostasis because of their participation in rapid water transportation across cell membranes (Jung *et al*, 1994). Alterations of water distribution in the brain may cause accumulation of intracellular water in neurons and glia, causing a cytotoxic brain edema. Brain edema is a significant factor leading to increased morbidity and mortality in many pathological processes of the CNS (Manley *et al*, 2000; Papadopoulos *et al*, 2002) and is a well-described phenomenon in HSVE (Schmutzhard, 2001). Furthermore, intracranial pressure monitoring is often necessary or even mandatory depending on the severity of brain edema during HSVE (Schmutzhard, 2001).

On the other hand, recent studies have described that the distribution of magnetic resonance imaging brain abnormalities in patients with neuromyelitis optica (NMO) correspond to sites of high aquaporin 4 (AQP4) expression (Pittock *et al*, 2006). The serum immunoglobulin G autoantibody (NMO-IgG) is a specific marker for NMO (Wingerchuk *et al*, 2006) and has been described to bind AQP4 selectively (Lennon, Kryzer *et al*, 2005). These findings suggest that NMO may represent the first example of AQP4 autoimmune channelopathy (Lennon *et al*, 2005). This could have wider implications because NMO-IgG– or anti-AQP4–associated neurological disorders could represent an emerging clinical entity (Giovannoni, 2006). It is necessary to study if other non–immune-mediated reversible AQP4 channelopaties exist (Giovannoni, 2006).

AQP4 is widely expressed in brain tissue, predominantly at brain-blood interfaces (Manley *et al*, 2000). The analysis of the expression pattern of AQP4 during HSVE might provide new information about the pathophysiology of this disease, which could eventually lead to novel therapeutic approaches aimed at limiting brain edema during the acute phase and structural damage during the chronic phase of disease. The role of AQP4 in the pathophysiology of HSVE has not been studied so far.

The aim of the present experimental work was to determine a possible role of AQP4 in an animal model of HSVE. We studied the temporal pattern of AQP4 mRNA expression and that of KIR 4.1, a membrane channel responsible for K^+ siphoning; of alpha-syntrophin, a protein associated to the distribution of AQP4 on astrocyte end-feet membrane domains adjacent to brain capillaries; of the structural protein glial fibrillary acid protein (GFAP), which is primarily expressed in astrocytes; and of aquaporin 1 (AQP1), a water channel expressed especially at the ventricular-facing of the choroid plexus epithelium.

Results

Infected animals presented the earliest clinical signs of disease 2 days after infection and clinical signs peaked at day 7. During the second week animals were severely affected. All infected animals scored at days 21 and 180 post inoculation were clinically normal again. Sham-inoculated animals had normal findings at all time points. Herpes simplex virus type 1 (HSV-1) DNA was present in the brain tissue of all examined infected animals. HSV-1 DNA was not detected in the brain tissue of sham-infected controls at any time. Viral burden peaked at day 7 post inoculation (Figure 1).

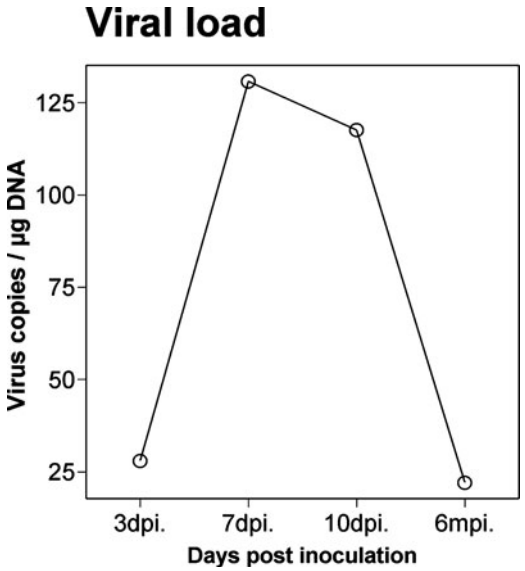

Figure 1 Viral burden. The viral burden in brain tissue was examined with nested PCR using serial dilutions of target DNA extracted from brain tissue as described previously (Lamadé *et al*, 1996; Martinez-Torres *et al*, 2004). Nested PCR was performed using two sets of oligodeoxynucleotide primers specific for the glycoprotein D gene of HSV-1. Amplified products (10 μl) were analyzed in agarose gels containing ethidium bromide and viewed with ultraviolet light. Each reaction included a negative control.

The basal expression of AQP4 was 2.9-fold higher in 6-month-old negative controls as compared to young negative controls (3.20 ± 1.39 versus 1.1 ± 0.41; $P < .0005$). A statistically significant 35% down-regulation of AQP4 expression was observed at day 7 post inoculation as compared to negative controls (0.71 ± 0.39 versus 1.1 ± 0.41; $P < .01$) (Figure 2A). AQP4 expression was not modified in infected animals at days 3 (2.05 ± 1.5 versus 1.1 ± 0.41; $P = .211$) and 10 post inoculation (1.47 ± 1.51 versus 1.1 ± 0.41; $P = 0.331$) as compared to negative controls. AQP4 expression was 5.5-fold up-regulated in infected animals as compared to negative controls 6 months after inoculation (17.66 ± 13.7 versus 3.20 ± 1.39; $P = .001$) (Figure 2B).

AQP1 basal expression was not modified with aging and remained stable in 6-month-old negative controls as compared to young negative controls (2.77 ± 2.28 versus 1.56 ± 1.63; $P = .262$) (Figure 3). AQP1 expression was not modified in infected animals during the acute phase of disease, at days 3 (1.23 ± 0.60 versus 1.56 ± 1.63; $P = .796$), 7 (0.56 ± 0.20

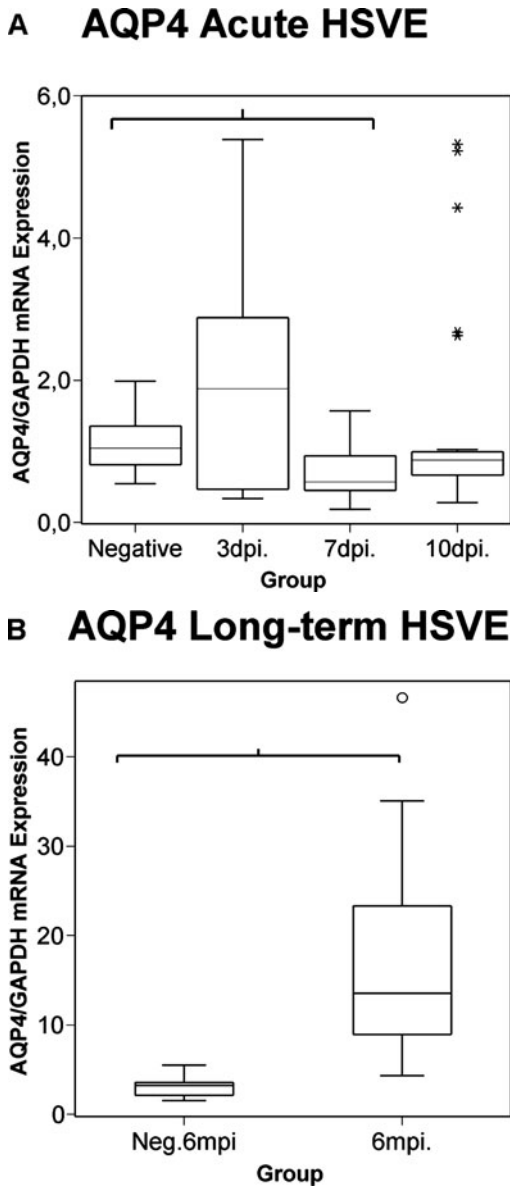

Figure 2 AQP4 expression during acute (**A**) and long-term (**B**) HSVE. A statistically significant 35% down-regulation of AQP4 was observed at day 7 post inoculation, and a significant 5.5× up-regulation 6 months post inoculation. Statistics were performed with the nonparametrical Kruskal-Wallis analysis, and the post hoc Mann-Whitney *U* test comparing infected animals with sham-inoculated age-matched negative controls. Data are presented as relative units (AQP4/GAPDH). The box represents the middle 50% of the data, the upper and lower ends of the box represent the upper and lower quartiles, respectively, and the horizontal line dividing the box represents the median. The whiskers represent the distribution and edges of the 95% percentile. Asterisks and circles represent extreme values. Statistical significance ($P < .05$) is depicted with a horizontal square bracket. Negative: negative controls in the acute phase; dpi: days post inoculation; mpi: months post inoculation; Neg.6mpi: negative controls 6 months post inoculation.

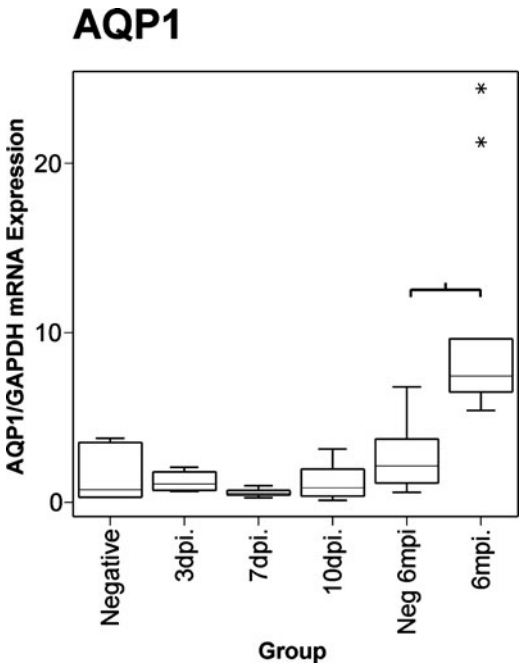

Figure 3 AQP1 expression in acute and long-term HSVE. Statistics were performed with the nonparametrical Kruskal-Wallis analysis and the post hoc Mann-Whitney *U* test comparing infected animals with sham-inoculated age-matched negative controls, and negative controls in the acute phase with negative controls in the chronic phase of disease. Data are presented as relative units (AQP1/GAPDH). The box represents the middle 50% of the data, the upper and lower ends of the box represent the upper and lower quartiles, respectively, and the horizontal line dividing the box represents the median. The whiskers represent the distribution and edges of the 95% percentile. Asterisks represent extreme values. Statistical significance ($P < .05$) is depicted with a horizontal square bracket. Negative: negative controls in the acute phase; dpi: days post inoculation; mpi: months post inoculation; Neg 6mpi: negative controls 6 months post inoculation.

versus 1.56 ± 1.63; $P = .399$), and 10 post inoculation (1.20 ± 1.11 versus 1.56 ± 1.63; $P = .606$) as compared to negative controls. A 3.76-fold up-regulation of AQP1 expression was observed in infected animals as compared to negative controls 6 months after inoculation (10.4 ± 6.74 versus 2.77 ± 2.28; $P = .005$) (Figure 3).

Basal KIR 4.1 expression was reduced 48% in 6-month-old negative controls as compared to young negative controls (0.26 ± 0.13 versus 0.5 ± 0.12; $P < .01$). We did not observe a statistically significant modification of KIR 4.1 expression in the acute phase of disease at days 3 (0.40 ± 0.21 versus 0.5 ± 0.12; $P = .796$) and 7 post inoculation (0.75 ± 0.43 versus 0.5 ± 0.12; $P = .223$), even though the expression tended to be 1.6-fold higher at day 10 post inoculation as compared to negative controls (0.80 ± 0.34 versus 0.5 ± 0.12; $P = .15$). KIR 4.1 expression was not modified in infected animals as compared to negative controls 6 months after inoculation (0.33 ± 0.17 versus 0.26 ± 0.13; $P = .386$) (Figure 4).

A significant 63% reduction of alpha-syntrophin basal expression was observed in 6-month-old negative controls as compared to young negative controls (0.26 ± 0.13 versus 0.7 ± 0.05; $P < .005$). There

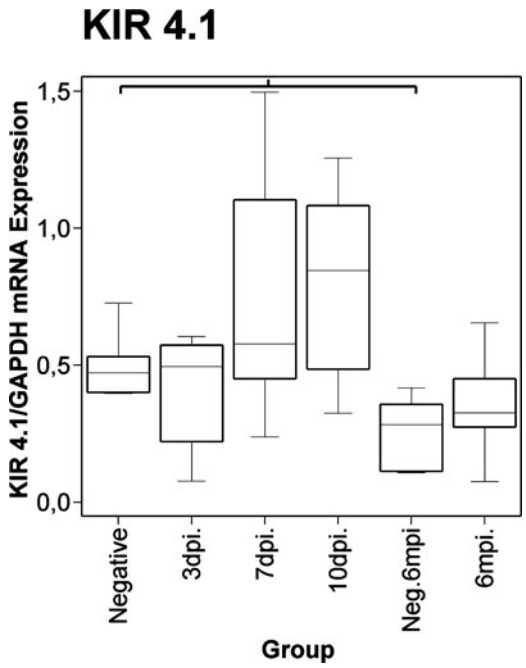

Figure 4 KIR 4.1 expression in acute and long-term HSVE. Statistics were performed with the nonparametrical Kruskal-Wallis analysis and the post hoc Mann-Whitney *U* test comparing infected animals with sham-inoculated age-matched negative controls, and negative controls in the acute phase with negative controls in the chronic phase of disease. Data are presented as relative units (KIR 4.1/GAPDH). The box represents the middle 50% of the data, the upper and lower ends of the box represent the upper and lower quartiles, respectively, and the horizontal line dividing the box represents the median. The whiskers represent the distribution and edges of the 95% percentile. Statistical significance ($P < .05$) is depicted with a horizontal square bracket. Negative: negative controls in the acute phase; dpi: days post inoculation; mpi: months post inoculation; Neg.6mpi: negative controls 6 months post inoculation.

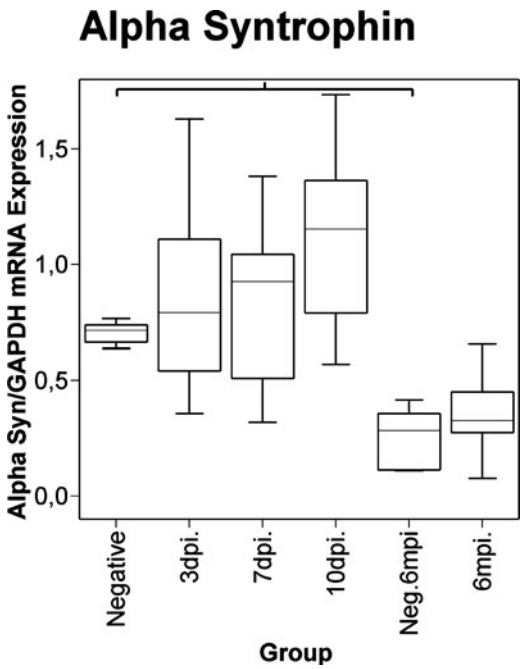

Figure 5 Alpha-syntrophin expression in acute and long-term HSVE. Statistics were performed with the nonparametrical Kruskal-Wallis analysis and the post hoc Mann-Whitney *U* test comparing infected animals with sham-inoculated age-matched negative controls, and negative controls in the acute phase with negative controls in the chronic phase of disease. Data are presented as relative units (alpha-syntrophin/GAPDH). The box represents the middle 50% of the data, the upper and lower ends of the box represent the upper and lower quartiles, respectively, and the horizontal line dividing the box represents the median. The whiskers represent the distribution and edges of the 95% percentile. Statistical significance ($P < .05$) is depicted with a horizontal square bracket. Negative: negative controls in the acute phase; dpi: days post inoculation; mpi: months post inoculation; Neg.6mpi: negative controls 6 months post inoculation.

was no statistically significant modification of alpha-syntrophin expression in the acute phase of disease at days 3 (0.85 ± 0.42 versus 0.7 ± 0.05; $P = .606$) and 7 post inoculation (0.82 ± 0.33 versus 0.7 ± 0.05; $P = .515$), even though the expression tended to be 1.6-fold higher at day 10 post inoculation as compared to negative controls (01.11 ± 0.4 versus 0.7 ± 0.05; $P = .121$). Alpha-syntrophin expression was not modified in infected animals as compared to negative controls 6 months after inoculation (0.33 ± 0.17 versus 0.25 ± 0.12; $P = .386$) (Figure 5).

GFAP basal expression was 4.64-fold higher in aging negative-control mice as compared to young negative controls (4.9 ± 5 versus 1.05 ± 0.64; $P = .015$). GFAP expression was not altered in infected animals during the acute phase of disease at days 3 (2.1 ± 2.4 versus 1.05 ± 0.64; $P = .519$), 7 (0.97 ± 0.16 versus 1.05 ± 0.64; $P = .574$) and 10 post-inoculation (1.88 ± 2.4 versus 1.05 ± 0.64, $P = 1.0$) or during the chronic phase of disease as compared to negative controls (3.6 ± 2.4 versus 4.9 ± 5.0; $P = .448$) (Figure 6).

Discussion

In this study we analyzed the temporal pattern of AQP4, AQP1, KIR 4.1, alpha-syntrophin and GFAP expression in the acute and chronic phases of experimental HSVE. The SJL-mouse model of HSVE resembles the pathological features (Hudson *et al*, 1991) and the focal structural MRI abnormalities of the disease in humans (Lamadé *et al*, 1996). The analyses of AQP4, AQP1, KIR 4.1, alpha-syntrophin and GFAP expression were performed with real-time (SYBR-Green) polymerase chain reaction (PCR), a highly sensitive method that provides an accurate mRNA quantification. This experimental model of HSVE affects the brain focally (Hudson *et al*, 1991; Lamadé *et al*, 1996). We consider that the observed phenomena could be even more drastic in the affected areas of the CNS, where viral replication takes place, such as described during human immunodeficiency virus (HIV) dementia (St Hilaire *et al*, 2005). Our results may be subject to a dilution effect given the focal nature of the experimental model, and because the

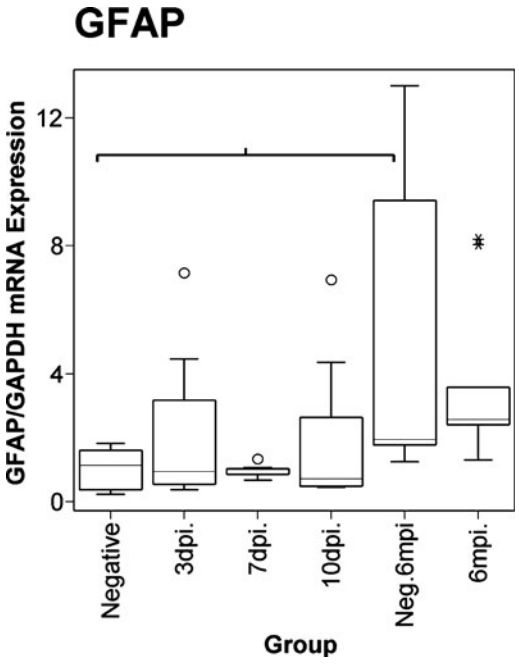

Figure 6 GFAP expression in acute and long-term HSVE. Statistics were performed with the nonparametrical Kruskal-Wallis analysis and the posthoc Mann-Whitney *U* test comparing infected animals with sham-inoculated age-matched negative controls, and negative controls in the acute phase with negative controls in the chronic phase of disease. Data are presented as relative units (GFAP/GAPDH). The box represents the middle 50% of the data, the upper and lower ends of the box represent the upper and lower quartiles, respectively, and the horizontal line dividing the box represents the median. The whiskers represent the distribution and edges of the 95% percentile. Asterisks and circles represent extreme values. Statistical significance ($P < .05$) is depicted with a horizontal square bracket. Negative: negative controls in the acute phase; dpi: days post inoculation; mpi: months post inoculation; Neg.6mpi: negative controls 6 months post inoculation.

observed regulation of gene expression was determined in whole brain tissue.

Aquaporins are a family of water channels that play a key role for water homeostasis in the CNS (AQP4) (Manley *et al*, 2000; Papadopoulos *et al*, 2002), and for the regulation of cerebrospinal fluid (CSF) production (AQP1) (Oshio *et al*, 2005). KIR 4.1 is a channel protein responsible for K^+ siphoning and has been observed to be coregulated with AQP4 in bacterial meningitis, cerebral contusions, and brain tumors (Saadoun *et al*, 2003). KIR 4.1 appears to buffer neurotoxic rises in extracellular K^+.

Our data revealed a statistically significant 35% down-regulation of AQP4 transcription in infected animals 7 days after inoculation as compared to negative controls, and a statistically significant 5.5× up-regulation of AQP4 mRNA levels in infected animals as compared to negative controls 6 months after inoculation. AQP1 transcription was not modified during the acute phase of HSVE. In contrast, we observed a 3.76× up-regulation of AQP1 transcription 6 months after inoculation.

An up-regulation of AQP4 has been described to correlate with an increase of edema formation in a model of focal cerebral ischemia (Lu and Sun, 2003). An enhanced AQP4 expression was observed after complement activation in brains of mice with lupus cerebritis (Alexander *et al*, 2003), during experimental pneumococcal meningitis (Papadopoulos and Verkman, 2005), and during other inflammatory processes of the brain (Aoki-Yoshino *et al*, 2005). In contrast, AQP4 expression was globally reduced after experimental traumatic brain injury (Kiening *et al*, 2002). Several studies suggest though that a redistribution of AQP4 expression on the cell membrane of astrocytes (Vajda *et al*, 2002; Warth *et al*, 2004) or uncoupled water transport from K^+ siphoning (Saadoun *et al*, 2003) might have a larger significance for the pathophysiology of brain edema than AQP4 regulation by itself.

The down-regulation of AQP4 transcription during the acute phase of experimental HSVE (at day 7 post inoculation) is similar to that observed after experimental traumatic brain injury (Kiening *et al*, 2002). Because AQP4 knockout mice present significantly reduced brain edema and better survival after acute water intoxication and ischemic stroke (Manley *et al*, 2000), the down-regulation of AQP4 expression in the early phase of traumatic brain injury was interpreted to reflect an endogenous protective mechanism aimed at reducing further glial swelling (Kiening *et al*, 2002). A similar mechanism could explain the findings during the acute phase of experimental HSVE. Nevertheless, the down-regulation of AQP4 at day 7 post inoculation seems to have been insufficient in order to modify the course of disease, because we did not observe a correlation with the clinical evolution of infected animals.

Furthermore, if AQP4 down-regulation were confirmed to be reproducible, experimental AQP4 inhibition could potentially be developed as a therapy for brain edema in a variety of disorders (Manley *et al*, 2000).

On the other hand, the exorbitant up-regulation of AQP4 in the chronic phase of HSVE seems to confirm previous studies observing AQP4 to be up-regulated in association with tissue damage in human glioblastoma (Warth *et al*, 2004) and other neoplastic diseases (Saadoun *et al*, 2003). AQP4 expression is increased in the mid frontal gyrus, an area of productive viral replication, during HIV dementia (St Hillaire *et al*, 2005). The fourfold range of AQP4 increased expression during HIV dementia, as determined with Western blot analysis, is similar to the observed 5.5-fold up-regulation during chronic HSVE. This increased AQP4 expression seems to be a response to proinflammatory stimuli, such as tumor necrosis factor (TNF)-α, thrombin, or matrix metalloproteinase 9 (MMP9), and may be a protective or a maladaptive response to inflammation (St Hillaire *et al*, 2005). This hypothesis is also plausible for HSVE, because proinflammatory stimuli such as the increased presence

of MMP9 have been described in the chronic phase of disease (Martinez-Torres *et al*, 2004). Interestingly, AQP4 mRNA expression was dramatically elevated in chronically infected animals as compared to their age-matched negative controls whereas GFAP levels in infected animals remained unchanged in the chronic phase of disease as compared to their age-matched negative controls. This fact strongly suggests that AQP4 up-regulation during chronic HSVE is a phenomenon independent from astrogliosis.

Furthermore, our observations could eventually have wider implications given that chronic progressive structural damage with areas of abnormal signal intensity in cranial MRI evolve despite appropriate antiviral treatment and very low viral replication, or no detectable viral replication whatsoever. These findings have been described in an experimental murine model of HSVE (Meyding-Lamadé *et al*, 1999b) as well as in patients who have survived HSVE (Meyding-Lamadé *et al*, 1999a). The nature of these chronic-progressive MRI changes has been interpreted to be virus independent. Autoimmune phenomena have been suggested to play a possible role for the development of these structural changes (Meyding-Lamadé *et al*, 2003). The exorbitant up-regulation of AQP4 observed in our experiments during the chronic phase of disease should be carefully studied in further experimental work in order to clarify if AQP4 could eventually play a role as a putative autoantigen.

AQP1 might have an important role in brain edema formation because AQP1 deletion leads to a reduction of osmotically induced water transport (Oshio *et al*, 2005). Even though a specific overexpression of AQP1 has been described in human brain tumors (Markert *et al*, 2001), the pathophysiological significance of this finding remains unknown. We observed a significant up-regulation of AQP1 in the chronic phase of HSVE. This finding requires further studies, particularly correlation with histopathology.

KIR 4.1 is a channel protein responsible for K^+ siphoning, and has often been found to be coregulated with AQP4 in previous studies in normal and pathological brain tissue (Saadoun *et al*, 2003). KIR.4.1 is thought to be associated with syntrophin protein complexes, which could have an important function to traffic channels to special subcellular locations (Leonoudakis *et al*, 2004). An uncoupling of the physiological coexpression of KIR 4.1 and AQP4 has been detected in inflammatory processes such as bacterial meningitis, brain tumors, and brain contusions (Saadoun *et al*, 2003). Our data did not show alteration of KIR 4.1 expression during the acute or chronic phase of HSVE, this fact appears to suggest an additional role for the uncoupling of AQP4 and KIR 4.1 expression in the pathophysiology of HSVE.

We observed that AQP4 expression is independent from that of alpha-syntrophin during long-term HSVE. Brain edema is attenuated in alpha-syntrophin knockout mice when stressed by transient cerebral ischemia, which is indicative of reduced water influx (Amiry-Moghaddam *et al*, 2003). Deletion of alpha-syntrophin causes a special pool of AQP4 to be reduced in perivascular and subpial membranes while other pools remain intact (Amiry-Moghaddam *et al*, 2004). On the other hand, there is interesting evidence that AQP4 can be redistributed in human glioblastoma due to the absence of agrin, which is important for the polarized distribution of AQP4 in astrocytes, and that AQP4 is closely associated to the dystrophin-dystroglican complex (Warth *et al*, 2004).

GFAP expression was higher in aging as compared to young negative-control animals. This reflects a larger proportion of GFAP mRNA in the absolute RNA pool of the aging brain and confirms the well-known phenomenon of astrogliosis during aging (Wu *et al*, 2005). AQP4 is mainly expressed in astroglial cells, and GFAP basal expression was interpreted in the experiments as an indicator of astrogliosis. AQP4 basal expression correlated to GFAP expression in negative-control animals. These findings strongly suggest that the elevation of AQP4 basal expression in the 6-month-old negative controls as compared to the young negative controls is correlated with astrogliosis.

AQP1 transcription was not altered with aging, which could reflect a constant mRNA pool from the choroid plexus epithelium. Contrary to this, KIR 4.1 and alpha-syntrophin transcription was significantly reduced in aging animals.

The current therapeutic options for the treatment of brain edema are limited (Manley *et al*, 2000). RNA interference (RNAi) of AQP4 has been proposed as an experimental therapeutic intervention for inflammatory processes of the CNS (Nicchia *et al*, 2003). Inhibition of AQP4 transcription could be a potential target to reduce brain edema, but there are still many questions surrounding the complex interactions of the molecules involved in water balance of the brain. The anchoring of AQP4 and alpha-syntrophin might be another potential target for intervention in brain edema (Amiry-Moghaddam *et al*, 2003).

Our data reveal the complex transcription pattern of AQP4, AQP1, KIR 4.1, alpha-syntrophin and GFAP during HSVE and suggest a role for AQP4 regulation in the pathophysiology of acute and long-term HSVE. Further studies should focus upon correlation with morphology and on the study of AQP4 modulation as a potential target for brain edema therapy during HSVE.

Methods

Animal model of herpes simplex virus encephalitis
All experiments were performed following an institutionally approved protocol in accordance with strict international regulations. Twenty-six female SJL-NBOM mice were maintained under artificial diurnal lighting conditions (12 h each of light and darkness) with free access to food and water. Mice

were at least 12 weeks old with a competent immune system, with an average weight of 24 g. Animals were briefly anesthetized and inoculated with 20 μl of intranasal virus suspension equivalent to 1×10^6 plaque-forming units, as previously described (Hudson *et al*, 1991; Lamadé *et al*, 1996; Martinez-Torres *et al*, 2004). Control animals were sham inoculated with sterile saline. The infectious agent was the neurovirulent wild-type HSV-1 strain F. The virus strain was propagated, passaged, and titrated as previously described (Lamadé *et al*, 1996). This experimental model resembles the morphology of human HSVE (Hudson *et al*, 1991; Lamadé *et al*, 1996; Martinez-Torres *et al*, 2004). Mice were clinically scored (Hudson *et al*, 1991) according to their appearance (normal or ruffled coat), posture (normal to permanently hunched), feeding habits, and neurological signs (agitation, circling, and presence of seizures) twice daily during the first 2 weeks after inoculation.

Infected animals were sacrificed at days 3 ($n = 4$), 7 ($n = 5$), 10 ($n = 4$), and 180 ($n = 5$) days post inoculation, and sham-inoculated negative-control animals at days 7 (n = 4) and 180 ($n = 4$) post inoculation. After sacrifice, mouse brains were microsurgically removed and snap frozen for further analysis.

DNA was isolated from 25 to 50 mg of murine brain tissue, which was homogenized with 1 ml of the organic solvent DNAzol (Gibco BRL, Eggenstein, Germany). After centrifugation the supernatant was decanted and the DNA pellet was washed, air dried, and thereafter solubilized in sterile water as described previously (Lamadé *et al*, 1996; Martinez-Torres *et al*, 2004). The concentration of isolated DNA was photometrically determined and samples stored at -20°C until further processing.

Nested polymerase chain reaction method

Nested polymerase chain reaction (PCR) was performed with two sets of oligodeoxynucleotide primers specific for the glycoprotein D gene of HSV-1 as described previously (Meyding-Lamadé *et al*, 1999b; Martinez-Torres *et al*, 2004). The primers amplify a 137-bp fragment of HSV-1. The sequences of the primers used for the first amplification reaction (HX 1 and HX 2) and the internal primers used for the second amplification reaction (HX 3 and HX 4) are depicted in Table 1. PCR was performed in an Omni Gene thermocycler (MWG Biotech, Ebersberg, Germany).

Ten microliters of the amplified product were analyzed by agarose gel electrophoresis (3% agarose, containing 0.3 μg/μl ethidium bromide) and viewed with ultraviolet light. Each reaction included a negative control.

Quantification of HSV-1 copies with a titration PCR assay

Viral copies were quantified with a standardized procedure established in our laboratory as previously described (Meyding-Lamadé *et al*, 1999b). Serial dilutions of aliquots of extracted DNA derived from brain tissue were tested in subsequent sets of eight identical amplification reactions. The aim was to obtain a maximum of two thirds of positive PCR reactions to make sure that a positive signal is equivalent to a single viral genome. As expected from a Poisson distribution, even in the presence of 50% positive reactions, two viral genomes are present before amplification in approximately one third of the total PCR assays (Simmonds *et al*, 1990). Reaction sets with more than five out of eight positive reactions were not taken into consideration to exclude samples that contained more than one single target molecule. Thus, the calculated viral load copies should be rather higher than indicated. The viral load was calculated as approximate number of HSV-1 copies per aliquot of DNA and adjusted to the number of copies per microgram DNA. We referred viral load to microgram DNA in order to take into account differences in individual brain weight and DNA extraction rates.

Table 1 Oligonucleotide primer sequences for the analysis of viral load with nested PCR

Primer	*Oligonucleotide sequence*
HX 1 (FW)	5′-ATC ACG CTA GCC CGG CCG TGT GAC A-3′
HX 2 (BW)	5′-CAT ACC GGA ACG CAC CAC ACA A-3′
HX 3 (FW)	5′-CCA TAC CGA CCA CAC CGA CGA-3′
HX 4 (BW)	5′-GGT AGT TGG TCG TTC GCG CTG AA-3′

Note. HX 1 and HX 2 were the primers used for the first amplification reaction, HX 3 and HX 4 are the internal primers used for the second amplification reaction. FW: sense primer; BW: antisense primer.

Analysis of the mRNA expression of AQP4, AQP1, KIR 4.1, alpha-syntrophin, and GFAP in brain tissue

Total RNA was isolated from brain tissue using RNA Clean (AGS, Heidelberg, Germany) according to the manufacturer's specifications, and reverse transcriptase–PCR (RT–PCR) was thereafter performed with random hexamers using a RNA Core Kit (Applied Biosystems, Weiterstadt, Germany). AQP4, AQP1, KIR 4.1, alpha-syntrophin, GFAP, and GAPDH sequences were amplified with a SYBR Green real-time quantitative PCR kit (Applied Biosystems, Weiterstadt, Germany) as follows: gene-specific, intron-spanning primers (Table 2) were designed using Primer Express software (Applied Biosystems). In order to correct for differences in the amount and quality of cDNA added to the reaction we used the housekeeping gene GAPDH as an endogenous reference. PCR was performed in four parallel reactions for each gene studied (AQP4, AQP1, KIR 4.1, alpha-syntrophin, GFAP, and GAPDH), per animal studied, using SYBR-Green reagents. Two hundred nanograms of cDNA were utilized for each PCR reaction. Each reaction mixture consisted of 1.25 U AmpliTaq Gold, 250 M deoxynucleotide triphosphates, 300 nM sense and 300 nM antisense primers in a total reaction

Table 2 Oligonucleotide primer sequences for the genes studied with real-time PCR

Primer	*Oligonucleotide sequence*
AQP4 FW	5′-GAA ACT GGG CAA ACC ACT GG-3′
AQP4 BW	5′-GCG ACG TTT GAG CTC CAC AT-3′
AQP1 FW	5′-ACA CCT GCT GGC GAT TGA CT-3′
AQP1 BW	5′-AGC CAA ATG ACC GGG CA-3′
KIR 4.1 FW	5′-CCG CGA TTT ATC AGA GCA GC-3′
KIR 4.1 BW	5′-TTA GCG ACC GAC GTC ATC TTG-3′
Alpha-syntrophin FW	5′-GAC AGT TGG TGG ATG GCT GTC-3′
Alpha-syntrophin BW	5′-TTC CAC GTG CAG GCT GTA GAC-3′
GFAP FW	5′-GGA ATT GCT GGA GGG CGA A-3′
GFAP BW	5′-TCC AGG CTG GTT TCT CGG A-3′
GAPDH FW	5′-CAT TGT GGA AGG GCT CAT GA-3′
GAPDH BW	5′-TCT TCT GGG TGG CAG TGA TG-3′

Note. FW: sense primer; BW: antisense primer.

volume of 30 μl. The temperature profile was programmed for the Gene Amp 5700 Sequence Detection System thermal cycler (Applied Biosystems) and was composed of two stages. Stage 1 corresponded to one initial cycle at 50°C for 2 min followed by 10 min at 95°C. Stage 2 consisted of 40 cycles at 95°C for 15 s and 60°C for 60 s. Expression of mRNA was measured as described previously (Martinez-Torres *et al*, 2004). A linear concentration-response curve was established by diluting pooled samples. The results for AQP4, AQP1, KIR 4.1, alpha-syntrophin and GFAP were normalized to those from GAPDH PCR in individual samples. The purity of the amplified product was confirmed with the dissociation curve and gel electrophoresis of selected samples.

Statistical analysis was performed using SPSS 14.0 software (SPSS, Chicago, IL, USA). Expression of AQP4, AQP1, KIR 4.1, alpha-syntrophin and GFAP mRNA was studied with the nonparametrical Kruskal-Wallis analysis and the post hoc Mann-Whitney *U* test comparing infected animals with sham-inoculated age-matched negative controls, and negative controls in the acute phase with negative controls in the chronic phase of disease. Results are presented in the text as mean relative units (gene/GAPDH) ± standard deviation (SD). The reported *P* values were two-tailed and $P < .05$ was considered statistically significant.

References

Alexander JJ, Bao L, Jacob A, Kraus DM, Holers VM, Quigg RJ (2003). Administration of the soluble complement inhibitor, Crry-Ig, reduces inflammation and aquaporin 4 expression in lupus cerebritis. *Biochim Biophys Acta* **1639:** 169–176.

Amiry-Moghaddam M, Frydenlund DS, Ottersen OP (2004). Anchoring of aquaporin-4 in brain: molecular mechanisms and implications for the physiology and pathophysiology of water transport. *Neuroscience* **129:** 999–1010.

Amiry-Moghaddam M, Otsuka T, Hurn PD, Traystman RJ, Haug FM, Froehner SC, Adams ME, Neely JD, Agre P, Ottersen OP, Bhardwaj A (2003). An alpha-syntrophin-dependent pool of AQP4 in astroglial end-feet confers bidirectional water flow between blood and brain. *Proc Natl Acad Sci U S A* **100:** 2106–2111.

Aoki-Yoshino K, Uchihara T, Duyckaerts C, Nakamura A, Hauw JJ, Wakayama Y (2005). Enhanced expression of aquaporin 4 in human brain with inflammatory diseases. *Acta Neuropathol (Berl)* **110:** 281–288.

Giovannoni G (2006). Neuromyelitis optica and anti-aquaporin-4 antibodies: widening the clinical phenotype. *J Neurol Neurosurg Psychiatry* **77:**1001–1002.

Hudson SJ, Dix RD, Streilein JW (1991). Induction of encephalitis in SJL mice by intranasal infection with herpes simplex virus type 1: a possible model of herpes simplex encephalitis in humans. *J Infect Dis* **163:** 720–727.

Jung JS, Bhat RV, Preston GM, Guggino WB, Baraban JM, Agre P (1994). Molecular characterization of an aquaporin cDNA from brain: candidate osmoreceptor and regulator of water balance. *Proc Natl Acad Sci U S A* **91:** 13052–13056.

Kiening KL, van Landeghem FK, Schreiber S, Thomale UW, von Deimling A, Unterberg AW, Stover JF (2002). Decreased hemispheric aquaporin-4 is linked to evolving brain edema following controlled cortical impact injury in rats. *Neurosci Lett* **324:** 105–108.

Lamadé UM, Lamade W, Hess T, Gosztonyi G, Kehm R, Sartor K, Hacke W (1996). A mouse model of herpes simplex virus encephalitis: diagnostic brain imaging by magnetic resonance imaging. *In Vivo* **10:** 563–568.

Lennon VA, Kryzer TJ, Pittock SJ, Verkman AS, Hinson SR (2005). IgG marker of optic-spinal multiple sclerosis binds to the aquaporin-4 water channel. *J Exp Med* **202:** 473–477.

Leonoudakis D, Conti LR, Anderson S, Radeke CM, McGuire LM, Adams ME, Froehner SC, Yates JR, 3rd, Vandenberg CA (2004). Protein trafficking and anchoring complexes revealed by proteomic analysis of inward rectifier potassium channel (Kir2.x)-associated proteins. *J Biol Chem* **279:** 22331–22346.

Lu H, Sun SQ (2003). A correlative study between AQP4 expression and the manifestation of DWI after the acute ischemic brain edema in rats. *Chin Med J (Engl)* **116:** 1063–1069.

Manley GT, Fujimura M, Ma T, Noshita N, Filiz F, Bollen AW, Chan P, Verkman AS (2000). Aquaporin-4 deletion in mice reduces brain edema after acute water intoxication and ischemic stroke. *Nat Med* **6:** 159–163.

Markert JM, Fuller CM, Gillespie GY, Bubien JK, McLean LA, Hong RL, Lee K, Gullans SR, Mapstone TB, Benos DJ (2001). Differential gene expression profiling in human brain tumors. *Physiol Genomics* **5:** 21–33.

Martinez-Torres FJ, Wagner S, Haas J, Kehm R, Sellner J, Hacke W, Meyding-Lamade U (2004). Increased presence of matrix metalloproteinases 2 and 9 in short- and

long-term experimental herpes simplex virus encephalitis. *Neurosci Lett* **368:** 274–278.

McGrath N, Anderson NE, Croxson MC, Powell KF (1997). Herpes simplex encephalitis treated with acyclovir: diagnosis and long term outcome. *J Neurol Neurosurg Psychiatry* **63:** 321–326.

Meyding-Lamadé U, Lamadé W, Kehm R, Oberlinner C, Fath A, Wildemann B, Haas J, Hacke W (1999a). Herpes simplex virus encephalitis: chronic progressive cerebral MRI changes despite good clinical recovery and low viral load—an experimental mouse study. *Eur J Neurol* **6:** 531–538.

Meyding-Lamadé UK, Lamadé WR, Wildemann BT, Sartor K, Hacke W (1999b). Herpes simplex virus encephalitis: chronic progressive cerebral magnetic resonance imaging abnormalities in patients despite good clinical recovery. *Clin Infect Dis* **28:** 148–149.

Meyding-Lamadé UK, Oberlinner C, Rau PR, Seyfer S, Heiland S, Sellner J, Wildemann BT, Lamadé WR (2003). Experimental herpes simplex virus encephalitis: a combination therapy of acyclovir and glucocorticoids reduces long-term magnetic resonance imaging abnormalities. *J NeuroVirol* **9:** 118–125.

Nicchia GP, Frigeri A, Liuzzi GM, Svelto M (2003). Inhibition of aquaporin-4 expression in astrocytes by RNAi determines alteration in cell morphology, growth, and water transport and induces changes in ischemia-related genes. *FASEB J* **17:** 1508–1510.

Oshio K, Watanabe H, Song Y, Verkman AS, Manley GT (2005). Reduced cerebrospinal fluid production and intracranial pressure in mice lacking choroid plexus water channel aquaporin-1. *FASEB J* **19:** 76–78.

Papadopoulos MC, Krishna S, Verkman AS (2002). Aquaporin water channels and brain edema. *Mt Sinai J Med* **69:** 242–248.

Papadopoulos MC, Verkman AS (2005). Aquaporin-4 gene disruption in mice reduces brain swelling and mortality in pneumococcal meningitis. *J Biol Chem* **280:** 13906–13912.

Pittock SJ, Weinshenker BG, Lucchinetti CF, Wingerchuk DM, Corboy JR, Lennon VA (2006). Neuromyelitis optica brain lesions localized at sites of high aquaporin 4 expression. *Arch Neurol* **63:** 964–968.

Saadoun S, Papadopoulos MC, Krishna S (2003). Water transport becomes uncoupled from K^+ siphoning in brain contusion, bacterial meningitis, and brain tumours: immunohistochemical case review. *J Clin Pathol* **56:** 972–975.

Schmutzhard E (2001). Viral infections of the CNS with special emphasis on herpes simplex infections. *J Neurol* **248:** 469–477.

Simmonds P, Balfe P, Peutherer JF, Ludlam CA, Bishop JO, Brown AJ (1990). Human immunodeficiency virus-infected individuals contain provirus in small numbers of peripheral mononuclear cells and at low copy numbers. *J Virol* **64:** 864–872.

St Hillaire C, Vargas D, Pardo CA, Gincel D, Mann J, Rothstein JD, McArthur JC, Conant K (2005). Aquaporin 4 is increased in association with human immunodeficiency virus dementia: implications for disease pathogenesis. *J NeuroVirol* **11:** 535–543.

Steiner I, Kennedy PG (1995). Herpes simplex virus latent infection in the nervous system. *J NeuroVirol* **1:** 19–29.

Vajda Z, Pedersen M, Fuchtbauer EM, Wertz K, Stodkilde-Jorgensen H, Sulyok E, Doczi T, Neely JD, Agre P, Frokiaer J, Nielsen S (2002). Delayed onset of brain edema and mislocalization of aquaporin-4 in dystrophin-null transgenic mice. *Proc Natl Acad Sci U S A* **99:** 13131–13136.

Warth A, Kroger S, Wolburg H (2004). Redistribution of aquaporin-4 in human glioblastoma correlates with loss of agrin immunoreactivity from brain capillary basal laminae. *Acta Neuropathol (Berl)* **107:** 311–318.

Wingerchuk DM, Lennon VA, Pittock SJ, Lucchinetti CF, Weinshenker BG (2006). Revised diagnostic criteria for neuromyelitis optica. *Neurology* **66:** 1485–1489.

Wu Y, Zhang AQ, Yew DT (2005). Age related changes of various markers of astrocytes in senescence-accelerated mice hippocampus. *Neurochem Int* **46:** 565–574.